The Role of Vimentin Intermediate Filaments in Cortical and Cytoplasmic Mechanics

Ming Guo,[†] Allen J. Ehrlicher,[†¶] Saleemulla Mahammad,[||] Hilary Fabich,[†] Mikkel H. Jensen,[†**] Jeffrey R. Moore,[**] Jeffrey J. Fredberg,[‡] Robert D. Goldman,[||] and David A. Weitz[†§*]

[†]School of Engineering and Applied Sciences, [‡]Program in Molecular and Integrative Physiological Sciences, School of Public Health, and [§]Department of Physics, Harvard University, Cambridge, Massachusetts; [¶]Beth Israel Deaconess Medical Center, Boston, Massachusetts; [||]Department of Cell and Molecular Biology, Northwestern University Feinberg School of Medicine, Chicago, Illinois; and **Department of Physiology and Biophysics, Boston University, Boston, Massachusetts

ABSTRACT The mechanical properties of a cell determine many aspects of its behavior, and these mechanics are largely determined by the cytoskeleton. Although the contribution of actin filaments and microtubules to the mechanics of cells has been investigated in great detail, relatively little is known about the contribution of the third major cytoskeletal component, intermediate filaments (IFs). To determine the role of vimentin IF (VIF) in modulating intracellular and cortical mechanics, we carried out studies using mouse embryonic fibroblasts (mEFs) derived from wild-type or vimentin$^{-/-}$ mice. The VIFs contribute little to cortical stiffness but are critical for regulating intracellular mechanics. Active microrheology measurements using optical tweezers in living cells reveal that the presence of VIFs doubles the value of the cytoplasmic shear modulus to ~10 Pa. The higher levels of cytoplasmic stiffness appear to stabilize organelles in the cell, as measured by tracking endogenous vesicle movement. These studies show that VIFs both increase the mechanical integrity of cells and localize intracellular components.

INTRODUCTION

Cells are regulated by complex biochemistry but are also inherently mechanical objects. The predominant elasticity of the cell arises from the cortex, which is the stiffest part of the cell. However, it is the cytoplasm that surrounds all the key organelles, and its mechanical properties are critical for a large number of cellular processes ranging from large-scale events such as maintenance of cell shape and generation of cell motility to more localized events such as mechanotransduction, signaling, and gene regulation (1). The cytoplasm is typically much less stiff than the cortex, although its mechanics have not been well quantified. In animal cells, the main contribution to cytoplasmic mechanics comes from the cytoskeleton, a scaffold that contains three major types of biopolymers: actin filaments, microtubules, and intermediate filaments (IFs). Both actin filaments and microtubules are dynamic polymers that are essential for the movement of cells and force generation (2). Their assembly is dependent on chemical energy derived from hydrolysis and they polymerize in a polar fashion, giving rise to highly dynamic structures that facilitate intracellular transport and cellular adaptation to changes in the external environment. In contrast, IF assembly is apolar and does not require the input of chemical energy from nucleoside triphosphate hydrolysis. The resulting filaments are generally considered to be more stable and mechanically robust than either actin filaments or microtubules (3–6).

IFs are important for maintaining the shape of cells and nuclei, and for regulating cellular motility and adhesion, and more than 80 distinct human diseases are associated with mutations in IF proteins. Even single-point mutations and deletions are manifest in severe diseases, including posterior cataracts (7), various muscle diseases (8), Alexander disease (9), blistering skin diseases (10), and neurodegenerative diseases (11,12). These diseases are usually related to incorrectly polymerized or organized IF structure, which in turn affects their network configuration in the cellular architecture (13). This suggests that in addition to possible changes in biochemical functionality, the mechanical properties of the IF networks may be dramatically altered. Recent in vitro experiments showed that cytoplasmic vimentin IFs (VIFs) can withstand significantly greater mechanical deformation than either microtubules or actin filaments (4), suggesting that vimentin may be a critical component in the mechanical integrity of cells. An in vitro study of IF networks revealed details of how IF assembly and crosslinking by divalent cations give rise to an elastic network (14). However, the contribution of IF to intracellular mechanics remains unknown.

In this work, we report the results of a direct measurement of the mechanical contribution of VIFs to the cell cortex and internal cytoplasm. To quantify the effect of VIFs, we used mouse embryonic fibroblasts (mEFs) from wild-type (WT) and vimentin knockout (Vim$^{-/-}$) mice, as shown in Fig.1. We used optical tweezers to perform active microrheology to probe the internal cytoplasmic mechanics, and found that VIFs increase the cytoplasmic stiffness by a factor of 2. The cytoplasmic stiffness is ~10 Pa in WT mEFs, whereas it is 5 Pa in the Vim$^{-/-}$ mEFs. To quantify the contribution of VIF to cytoplasmic dynamics, we tracked the fluctuating intracellular movement of endogenous vesicles. We found

Submitted June 27, 2013, and accepted for publication August 22, 2013.

*Correspondence: weitz@seas.harvard.edu

Editor: David Piston.

0006-3495/13/10/1562/7 $2.00

http://dx.doi.org/10.1016/j.bpj.2013.08.037

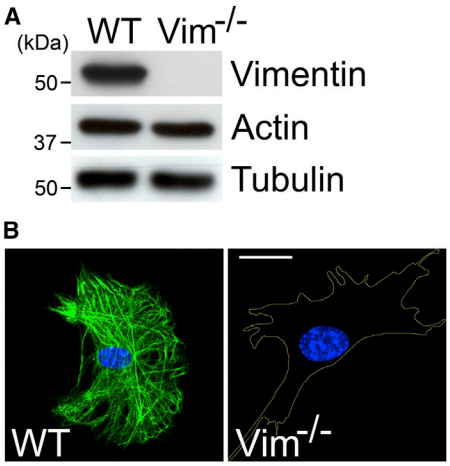

FIGURE 1 Analysis of control (WT) and VIM$^{-/-}$ mEF cells. (*A*) Immunoblot analyses of cell lysates from WT and VIM$^{-/-}$ mEFs using antibodies to vimentin, actin, and tubulin. Representative blots from three experiments are shown. (*B*) Immunofluorescence using antibodies against vimentin in control (WT, *left*) and VIM$^{-/-}$ (*right*) mEFs. The cell boundary in VIM$^{-/-}$ mEFs is represented by the yellow line. Representative images from three experiments are shown. Scale: 10 μm. To see this figure in color, go online.

that the presence of VIF reduces intracellular movement and localizes these organelles. Using optical magnetic twisting cytometry (OMTC) (15–17), we also directly measured the cortical stiffness in both cell types. Interestingly, in contrast to its effect on cytoplasmic stiffness, VIFs do not significantly change the cortical stiffness of the cell. These mechanical contributions highlight the role of VIFs as a significant and important structural component of cytoplasm.

MATERIALS AND METHODS

Cell culture

WT and Vim$^{-/-}$ mEFs (18) were cultured in Dulbecco's minimal essential medium supplemented with 10% fetal calf serum, 5 mM nonessential amino acids (NEAA), 100 U/ml penicillin, and 100 μg/ml streptomycin, and maintained under 5% CO_2 at 37°C in a humidified incubator. Cells were passaged onto glass-bottom cell culture dishes containing collagen-I-coated coverslips and allowed to grow overnight before experiments were conducted.

SDS-PAGE and immunoblotting

SDS-PAGE and immunoblotting were performed as previously described (19). Briefly, cells were grown in 100 mm culture dishes and lysed in Laemmli sample buffer. Proteins separated by SDS-PAGE were transferred onto nitrocellulose membranes (Protran nitrocellulose membrane; Whatman) and probed with the following antibodies: mouse anti-vimentin 1:7000 (clone v9), mouse anti-alpha tubulin 1:6000 (Sigma, St. Louis, MO), and mouse monoclonal anti-actin (clone c4, 1:8000; Millipore, Billerica, MA). Peroxidase-conjugated goat anti-mouse (Jackson ImmunoResearch, West Grove, PA) was used at 1:10,000 dilution. Blots were developed by SuperSignal West Pico Chemiluminescent Substrate (Thermo Scientific, Rockford, IL). X-ray films were used to image the chemiluminescence signals.

Immunofluorescence, microscopy, and image processing

Immunofluorescence and microscopy were carried out as previously described (20). Briefly, cells were plated on glass coverslips, grown overnight, and fixed in ice-cold methanol. The fixed cells were immunostained with chicken anti-vimentin primary antibody (Covance, Princeton, NJ) (1:400 dilution in PBS supplemented with 0.01% Tween 20 (PBST)) and Alexa 488 conjugated goat anti-chicken secondary antibody (Molecular Probes/Invitrogen, Carlsbad, CA; 1:400 dilution in PBST). Nuclei were stained with Hoechst 33258 (Invitrogen, Carlsbad, CA). Fixed and stained cells were mounted on glass slides and imaged with a Zeiss Confocal LSM510 META microscope with oil immersion objective lenses (Plan-Apochromat, 63× and 100×, 1.40 NA; Carl Zeiss). Images were processed as previously described (18).

Cytoplasmic material properties measured using optical tweezers

To optically trap and manipulate 500 nm beads in the cytoplasm of mEFs, we steered the beam from a variable-power Nd:YAG solid-state laser (4 W, 1064 nm; Spectra Physics, Mountain View, CA) through a series of Keplerian beam expanders to overfill the back aperture of a 100× 1.3 numerical aperture microscope objective (Nikon S-fluor; Nikon, Tokyo, Japan). To steer the beam and manipulate the trapped bead, we used two acousto-optic deflectors (NEOS Technologies, Melbourne, FL). Using a custom-written Labview program (National Instruments, Austin, TX), we manipulated the acousto-optic deflectors to control the beam in the plane of the microscope glass slide. For detection, the bead was centered on a high-resolution, position-detection quadrant detector (MBPS; Spectral Applied Research, Richmond Hill, ON, Canada) and illuminated using bright-field illumination from a 75 W Xe lamp. The linear region of the detector was calibrated by trapping a bead identical to those used in the cells in water and moving it across the detector using the acousto-optic deflectors in known step sizes. The trap stiffness was calibrated from the mean-squared Brownian motion of a trapped bead in water at various laser power settings using the principle of energy equipartition as previously described (21).

Once it was calibrated, the laser trap was used to optically trap and manipulate beads intracellularly. The laser power at the sample was roughly 200 mW, corresponding to a trap stiffness of 0.05 pN/nm for the beads used. Trapped beads were oscillated across a frequency range of 1–100 Hz using the acousto-optic deflectors, and the laser position and bead displacement (from which the elastic and viscous shear moduli were determined) were recorded simultaneously. By measuring the resultant displacement of the bead, $x(\omega)$, subjected to an applied sinusoidal trap oscillation with a force F at frequency ω, we were able to extract the effective spring constant, $K(\omega) = F(\omega)/x(\omega)$, for a given intracellular environment. For materials with dissipation, the displacement, x, and force, f, are not in phase, which results in a complex spring constant. For a homogeneous, incompressible viscoelastic material, this spring constant is related to a complex modulus, $G = G' + iG''$, through a generalization of the Stokes relation $K = 3\pi Gd$ (22), where d is the bead diameter.

Tracking vesicle movements

To monitor intracellular movement, we tracked the motion of endogenous vesicles that budded off from cellular membranes. These refractive vesicles were visualized by bright-field microscopy using a 633-nm laser and a 63×/1.2NA water immersion lens on a Leica TSC SP5 microscope. To avoid cell-boundary effects, only vesicles located away from the thin lamellar region and the nucleus, and more than ~1 μm deep within the cell were analyzed. This selection of vesicles avoided any interactions with the mechanically distinct cell cortex and nucleus. The trajectories of the vesicles were recorded every 18 ms for 30 s. Vesicle centers were determined

by calculating the centroid of the vesicle's brightness distributions in each image with an accuracy of 20 nm. Vesicle trajectories were tracked to calculate the time and ensemble-averaged mean-square displacement (MSD), $<\Delta r^2(\tau)>$, where $\Delta r(\tau) = r(t+\tau) - r(t)$.

Cortical stiffness measurements

The mechanical properties of the cell cortex were probed using OMTC, which is a high-throughput tool for measuring adherent cell mechanics with high temporal and spatial resolution (15–17). For these measurements, cells were plated on collagen-I-coated plastic dishes at a density of ~10 cells per mm^2 and allowed to grow overnight. Then 4.5-μm ferromagnetic beads (produced as described previously (23)) coated with poly-L-lysine (4 kDa) were incubated with the cells for 20 min to achieve strong coupling to the cell surface (poly-L-lysine binds to the cells nonspecifically and tightly, but does not induce active remodeling of the cytoskeleton (24)). Unbound beads were removed by gentle washing, leaving a few beads attached to each cell. The dish was mounted on a heated microscope stage to maintain 37°C. Beads were magnetized by a strong, horizontal magnetic field and then twisted by an oscillatory vertical magnetic field at frequencies of $f = 0.1$–1000 Hz and amplitudes of ~25–50 Gauss. The motions of hundreds of beads in a field of view were recorded with a CCD camera (C4742-95-12ERG; Hamamatsu) mounted on an inverted microscope (DM IRE2; Leica) with a 10× objective, and the beads' positions were determined in real time with >10 nm accuracy by means of an intensity-weighted center-of-mass algorithm. The ratio between the torque and bead motion thus defines an apparent stiffness for a cell, which has the unit Pa/nm. A series of geometric factors based on finite-element models that take into account the cell thickness and bead-cell coupling can be used to convert the apparent stiffness into shear modulus of the cell, as discussed previously (15–17). The bead-cell contact geometry was characterized by confocal fluorescence microscopy of labeled live cells; beads were embedded ~30% deep in WT and Vim$^{-/-}$ mEFs (standard deviations (SDs) = ~5%), so the same geometric factors were used. Previous measurements of cortical stiffness obtained by OMTC agree with values obtained by other methods, such as atomic force microscopy (AFM) (25).

RESULTS

VIFs stiffen the cytoplasm

To measure cytoplasmic mechanics, we performed active microrheology using optical tweezers on single polystyrene particles that had been endocytosed by WT or Vim$^{-/-}$ mEFs and were randomly distributed within the cytoplasm. These 500-nm-diameter particles were covered with lipid layers during endocytosis and thus could be transported along microtubules; however, most of the time these particles displayed random movement. To focus on the contribution of VIF to cytoplasmic mechanics, we measured only the movement of particles located away from both the thin lamellar region and the nucleus, thereby avoiding these mechanically distinct regions of the cell. About 8 hr after addition of the particles, we used a 1064 nm solid-state laser to trap a single bead and generate a sinusoidally oscillating force F on the trapped particle (see Materials and Methods section). By measuring the displacement of the trapped particle, $x(\omega)$, resulting from the applied oscillating force at frequency ω, we were able to extract the effective spring constant, $K(\omega) = F(\omega)/x(\omega)$, for the intracellular environment. For purely elastic materials, displacement and force are in phase, whereas for materials with viscous dissipation, the displacement and force are not in phase. This enabled us to determine both the elastic spring constant, G', and the viscous loss component, G''.

Our active microrheology measurements in the cytoplasm exhibit a displacement that is almost in phase with the oscillating force, as shown in Fig. 2 *B*; thus, the micromechanical environment in the cytoplasm of mEF cells is predominantly elastic rather than viscous. Moreover, the measured elastic modulus G' is consistently larger than the loss modulus G'' over the frequency range investigated (from 1 to 100 Hz). This shows that the cytoplasm of mEFs is an elastic gel instead of a viscous fluid, when measured on submicron length scales. Furthermore, both the elastic modulus G' and the loss modulus G'' increase with frequency, following a power-law form, $|G(\omega)| \sim \omega^{\beta}$, with $\beta \approx 0.25$. This observation agrees with the power-law rheology observed previously for living cells and biopolymer networks (15,26). This value is also in agreement with those obtained when a cell is stretched between microplates (β ~0.2–0.3) (27) or is locally externally deformed at the cortex using either magnetic tweezers or AFM (β~0.2) (15,28).

Although both WT and VIM$^{-/-}$ mEFs show similar frequency-dependent behavior, the cytoplasmic elastic modulus, G', of WT mEFs is larger than that of VIM$^{-/-}$ mEFs, as shown in Fig. 3 *A*. Specifically, at 1 Hz the

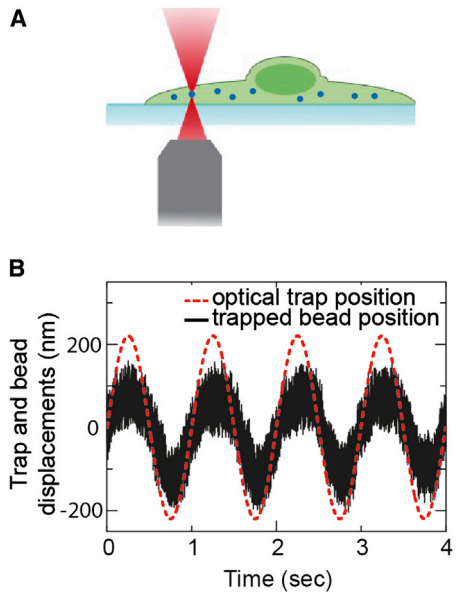

FIGURE 2 Optical-tweezers measurement of intracellular mechanics. (*A*) Schematic of the optical tweezer experiment. PEG-coated inert particles (500 nm) are endocytosed into mEF cells and are then trapped and manipulated by a spatially sinusoidal oscillating optical trap, which generates a force F at frequency ω. The frequency-dependent complex spring constant is calculated by measuring the resultant displacement x of the bead in the trap oscillation, as F/x. (*B*) Typical displacements of the trapped bead and the optical trap oscillating at 1 Hz. To see this figure in color, go online.

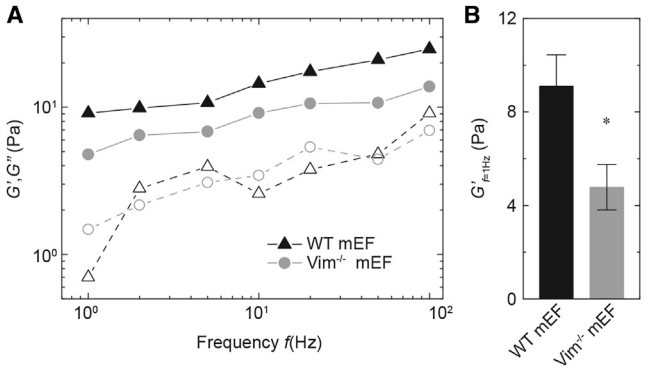

FIGURE 3 Active microrheology with optical tweezers controlling 500 nm endocytosed beads in the cytoplasm of mEFs. (*A*) Frequency-dependent cytoplasmic elastic moduli G' (*solid symbols*) and loss moduli G'' (*open symbols*) of the WT and Vim$^{-/-}$ mEFs. The cytoplasm of the WT mEFs (*triangles*) is stiffer than that of the Vim$^{-/-}$ mEFs (*circles*). (*B*) Cytoplasmic elastic moduli in the WT and Vim$^{-/-}$ mEFs at 1 Hz. Error bars: SEM ($*p < 0.05$).

cytoplasm of WT mEFs is twice as stiff as that of VIM$^{-/-}$ mEFs; thus, the presence of vimentin increases the cytoplasmic elastic modulus from ~5 Pa to 9 Pa (Fig. 3 *B*). However, the loss modulus G'' is not significantly different between the WT and VIM$^{-/-}$ cells over the investigated frequency range; the loss tangent, as defined by G''/G' which represents the relative dissipation of materials, is roughly twice as large for the VIM$^{-/-}$ cells, indicating that the presence of vimentin also reduces energy dissipation in the cytoplasm. The significant difference in cytoplasmic moduli between WT and VIM$^{-/-}$ mEFs reflects the contribution of VIF to the intracellular stiffness, suggesting that vimentin is a crucial structural cellular component within the cytoplasm.

VIFs reduce intracellular fluctuating movement

VIFs also affect intracellular activity. To investigate how intracellular dynamics are influenced by cytoplasmic mechanics due to the VIF network, we focused on the movement of endogenous vesicles, small organelles that bud off from cellular membranes to form submicron carriers that facilitate intracellular transport of materials. We used bright-field microscopy to directly track the movement of such vesicles in WT and VIM$^{-/-}$ mEFs. We excluded trajectories from the thin actin-rich lamellar region and the mechanically distinct nucleus, focusing instead on the midplane of the cells where VIFs are typically distributed. Occasionally, the motion was clearly directed, with vesicles moving along a straight path at a constant velocity, reflecting vectorial transport along microtubules by motors. However, the majority of the motion appeared to be random, and the MSD increased linearly in time, reflecting the diffusive-like nature of the motion (29). Although the trajectories of vesicles in both WT and VIM$^{-/-}$ mEFs indicate random movements, the vesicles in VIM$^{-/-}$ mEFs move farther over the same timescale, as shown in Fig. 4 *A*. Quantifying the trajectories by plotting the MSD of these vesicles reveals that although both of them increase linearly with time, the vesicles move an order of magnitude faster in the VIM$^{-/-}$ mEFs as compared with the control WT mEFs (Fig. 4 *B*). Additionally, the slope of the MSD is slightly larger for the VIM$^{-/-}$ cells (~1.27) than for the WT cells (~1.21). This increased movement in VIM$^{-/-}$ cells is consistent with previous observations of the movements of mitochondria (30), I melanosomes (31), the Golgi apparatus (32,33), and other organelles (34,35), suggesting that VIFs may contribute to determining the localization of a variety of different organelles.

VIFs do not change cortical stiffness

To determine whether VIFs contribute to the cell cortical stiffness, we measured the deformation of individual mEFs resulting from forces applied through a magnetic bead bound on the cell surface, a technique called OMTC (see diagram in Fig. 5 *A*). This technique has been used extensively to measure material properties of cells (15,16) and the results agree quantitatively with measurements obtained with other methods, such as AFM. We probed the force-deformation relationship over four decades of frequency range using OMTC, and calculated the elastic shear modulus, G', and the viscous loss component, G'', of the cell cortex from those results (see Materials and Methods). The OMTC measurement reveals that the cell cortexes of both WT and VIM$^{-/-}$ mEFs are solid-like, with an elastic modulus G' much larger than the loss modulus G'' over the frequency range investigated (from 0.1 to 1000 Hz). The magnitude of shear moduli determined from the cortical OMTC measurements is two orders of magnitude larger than that of the cytoplasm. However, both G' and G'' of the cortex increase with frequency in a power-law form, as $|G(\omega)| \sim \omega^{\beta}$, with $\beta \approx 0.2$. Both the power-law form and the value of β are in accord with the behavior of the cytoplasm, as well as with previous cortical measurements (15,27,28). Interestingly, however, there is no significant difference in either G' and G'' between WT and VIM$^{-/-}$ mEFs (Fig. 5 *B*), suggesting that VIFs do not affect the material properties of the cell cortex, which is mainly composed of actin filaments. Thus, these measurements highlight the specific structural role of VIF in the cytoplasm rather than the cortex.

DISCUSSION

Eukaryotic cells withstand a wide range of passive and active forces, and they resist deformation, localize organelles, and maintain shape under external forces. This mechanical robustness relies critically on the cytoskeleton, which is composed of filamentous polymers and regulatory

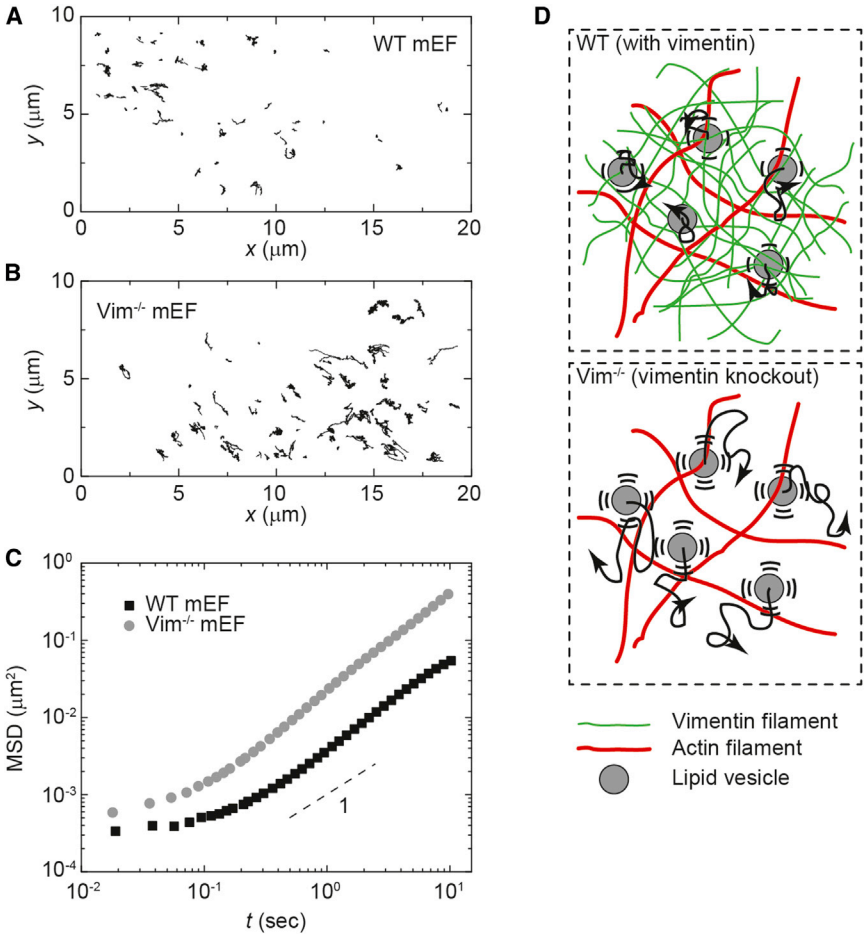

FIGURE 4 Intracellular movement of endogenous vesicles inside WT and Vim$^{-/-}$ mEFs. (*A* and *B*) Ten-second trajectories of endogenous vesicles in the cytoplasm of (*A*) WT mEFs and (*B*) Vim$^{-/-}$ mEFs. (*C*) Calculation of the MSD of vesicles shows that vesicles move faster in the Vim$^{-/-}$ mEFs than in the WT mEFs. (*D*) Illustration of random vesicle movement in networks with and without vimentin. In the WT cells, the vimentin network constrains the diffusive-like movement of organelles; in the VIM$^{-/-}$ cells, organelles move more freely. To see this figure in color, go online.

proteins. The cell cortex forms a stiff shell that is mechanically dominated by a dense actin meshwork, which together with myosin II creates a responsive and dynamic structure. Beneath the cortex, the cytoplasm is much softer because it is composed of dilute structural proteins, organelles, and cytosol. These two distinct cytoskeletal regions create a composite network that transmits mechanical signals from the extracellular matrix to the nucleus (36,37) while spatially organizing and mechanically protecting cellular components (38). Therefore, cytoplasmic mechanics play a key role in many aspects of cell function, and mechanical defects may be directly related to pathology (39). IFs, as one of the three major filamentous polymers of the cytoskeleton, are known to be involved in regulating cell movement, contraction, and internal transport (40–42); however, their role in cytoplasmic mechanics has not yet been investigated. Our active microrheology measurements show that the cytoplasmic shear modulus of the WT mEFs is ~80% larger than that of the VIM$^{-/-}$ mEFs. In comparison with the WT mEFs, the VIM$^{-/-}$ mEFs have the same amount of actin and tubulin, but no VIF (Fig. 1); therefore, the difference in our measurements reflects the specific mechanical contribution of VIF. At 1 Hz, vimentin increases the cytoplasmic shear modulus from 5 Pa to 9 Pa (Fig. 3). By comparison, in vitro rheology measurements of VIF networks indicate an elastic shear modulus of a few pascals (26,43). In contrast, vimentin does not have any measurable effect on the cortical stiffness, which is two orders of magnitude greater than the cytoplasmic stiffness (Fig. 5 *B*). The substantially higher stiffness and the negligible contribution of vimentin in the cortex are both attributable to the dominance of the actin-rich structure of the cortex. Within the cytoplasm, actin network structures are less abundant, and therefore vimentin plays a critical role in a variety of properties. In addition to mechanical changes, cells without VIF have different shapes, lower motility, and weaker adhesion (40–42). Our results complement these findings by providing evidence that VIFs also contribute to the intracellular mechanics, suggesting that VIFs are essential for the structural integrity of cells.

In addition to contributing to cell mechanics, another major role of cytoplasmic VIFs is to spatially organize the contents of the cell (38). Eukaryotic cells have a wide variety of organelles that serve different functions, and these organelles distribute across the cell according to changing physiological needs and in addition are subjected to constant fluctuations due to thermal agitation and active forces (29). By tracking the movement of submicron lipid vesicles, we

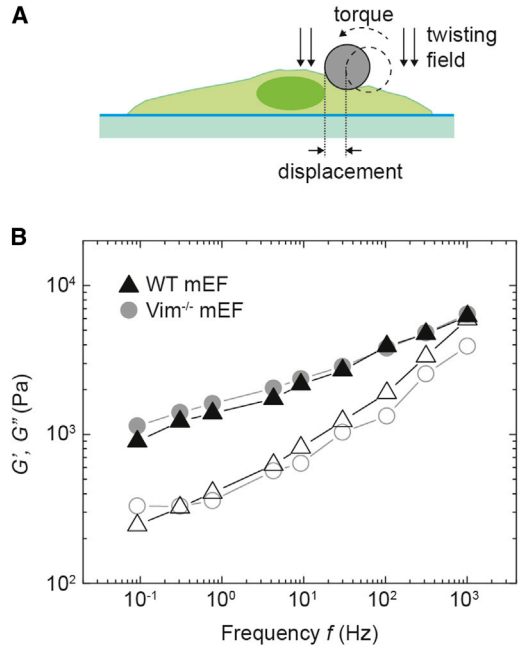

FIGURE 5 Cell cortical material properties of WT and VIM$^{-/-}$ mEFs measured with OMTC. (*A*) Schematic of the OMTC measurement. A magnetic field introduces a torque that causes the 4.5-μm ferromagnetic bead to rotate and to deform the cell cortex to which it is bound. (*B*) Elastic (G', *solid symbol*), and loss (G'', *open symbol*) moduli for WT (*black triangles*) and Vim$^{-/-}$ (*gray circles*) mEFs cultured overnight on collagen-I-coated rigid plastic dishes, as measured by OMTC. Approximately 100 single cells are measured for each cell type. To see this figure in color, go online.

show that the VIF network indeed reduces these random fluctuation of vesicles, in agreement with observations that the movement of other organelles, such as mitochondria, is confined by VIFs (30). These results suggest that cytoplasmic VIF, as a structural polymer, also helps to localize organelles in cells. This might be a direct consequence of the increase of cytoplasmic stiffness. Since VIFs increase the cytoplasmic stiffness by ~80%, this reduces the random movement of contents that are integrated in the cytoplasmic network, and effectively localizes organelles, such as the nucleus and endoplasmic reticulum. This highlights how a structural biopolymer such as VIF can have an extensive and unexpected impact through its mechanical properties.

We thank F. Mackintosh and A. Rowat for many helpful discussions, and E. Kuczmarski for a critical reading of the manuscript. This work was supported by the National Institutes of Health (P01GM096971) and the Harvard Materials Research Science and Engineering Center (DMR-0820484).

REFERENCES

1. Alberts, B., A. Johnson, J. Lewis, M. Raff, K. Roberts, and P. Walter. 2007. Molecular Biology of the Cell. Garland Science, New York.
2. Carlier, M. F. 1989. Role of nucleotide hydrolysis in the dynamics of actin filaments and microtubules. *Int. Rev. Cytol.* 115:139–170.
3. Herrmann, H., H. Bär, …, U. Aebi. 2007. Intermediate filaments: from cell architecture to nanomechanics. *Nat. Rev. Mol. Cell Biol.* 8:562–573.
4. Janmey, P. A., U. Euteneuer, …, M. Schliwa. 1991. Viscoelastic properties of vimentin compared with other filamentous biopolymer networks. *J. Cell Biol.* 113:155–160.
5. Sivaramakrishnan, S., J. V. DeGiulio, …, K. M. Ridge. 2008. Micromechanical properties of keratin intermediate filament networks. *Proc. Natl. Acad. Sci. USA.* 105:889–894.
6. Qin, Z., L. Kreplak, and M. J. Buehler. 2009. Hierarchical structure controls nanomechanical properties of vimentin intermediate filaments. *PLoS ONE.* 4:e7294.
7. Bornheim, R., M. Müller, …, T. M. Magin. 2008. A dominant vimentin mutant upregulates Hsp70 and the activity of the ubiquitin-proteasome system, and causes posterior cataracts in transgenic mice. *J. Cell Sci.* 121:3737–3746.
8. Gallanti, A., A. Prelle, …, G. Scarlato. 1992. Desmin and vimentin as markers of regeneration in muscle diseases. *Acta Neuropathol.* 85:88–92.
9. Brenner, M., A. B. Johnson, …, A. Messing. 2001. Mutations in GFAP, encoding glial fibrillary acidic protein, are associated with Alexander disease. *Nat. Genet.* 27:117–120.
10. Chamcheu, J. C., I. A. Siddiqui, …, H. Mukhtar. 2011. Keratin gene mutations in disorders of human skin and its appendages. *Arch. Biochem. Biophys.* 508:123–137.
11. Perrot, R., R. Berges, …, J. Eyer. 2008. Review of the multiple aspects of neurofilament functions, and their possible contribution to neurodegeneration. *Mol. Neurobiol.* 38:27–65.
12. Perrot, R., and J. Eyer. 2009. Neuronal intermediate filaments and neurodegenerative disorders. *Brain Res. Bull.* 80:282–295.
13. Omary, M. B., P. A. Coulombe, and W. H. I. McLean. 2004. Intermediate filament proteins and their associated diseases. *N. Engl. J. Med.* 351:2087–2100.
14. Hofmann, I., H. Herrmann, and W. W. Franke. 1991. Assembly and structure of calcium-induced thick vimentin filaments. *Eur. J. Cell Biol.* 56:328–341.
15. Fabry, B., G. N. Maksym, …, J. J. Fredberg. 2001. Scaling the microrheology of living cells. *Phys. Rev. Lett.* 87:148102.
16. Fabry, B., G. N. Maksym, …, J. J. Fredberg. 2001. Selected contribution: time course and heterogeneity of contractile responses in cultured human airway smooth muscle cells. *J. Appl. Physiol.* 91:986–994.
17. Mijailovich, S. M., M. Kojic, …, J. J. Fredberg. 2002. A finite element model of cell deformation during magnetic bead twisting. *J. Appl. Physiol.* 93:1429–1436.
18. Mahammad, S., S. N. Murthy, …, R. D. Goldman. 2013. Giant axonal neuropathy-associated gigaxonin mutations impair intermediate filament protein degradation. *J. Clin. Invest.* 123:1964–1975.
19. Grin, B., S. Mahammad, …, R. D. Goldman. 2012. Withaferin a alters intermediate filament organization, cell shape and behavior. *PLoS ONE.* 7:e39065.
20. Helfand, B. T., M. G. Mendez, …, R. D. Goldman. 2011. Vimentin organization modulates the formation of lamellipodia. *Mol. Biol. Cell.* 22:1274–1289.
21. Veigel, C., M. L. Bartoo, …, J. E. Molloy. 1998. The stiffness of rabbit skeletal actomyosin cross-bridges determined with an optical tweezers transducer. *Biophys. J.* 75:1424–1438.
22. Mizuno, D., C. Tardin, …, F. C. Mackintosh. 2007. Nonequilibrium mechanics of active cytoskeletal networks. *Science.* 315:370–373.
23. Moller, W., C. Roth, and W. Stahlhofen. 1990. Improved spinning top aerosol generator for the production of high concentrated ferrimagnetic aerosols. *J. Aerosol. Sci.* 21:S657–S660.
24. Zhou, E. H., X. Trepat, …, J. J. Fredberg. 2009. Universal behavior of the osmotically compressed cell and its analogy to the colloidal glass transition. *Proc. Natl. Acad. Sci. USA.* 106:10632–10637.

25. Byfield, F. J., Q. Wen, …, P. A. Janmey. 2009. Absence of filamin A prevents cells from responding to stiffness gradients on gels coated with collagen but not fibronectin. *Biophys. J.* 96:5095–5102.

26. Lin, Y. C., C. P. Broedersz, …, D. A. Weitz. 2010. Divalent cations crosslink vimentin intermediate filament tail domains to regulate network mechanics. *J. Mol. Biol.* 399:637–644.

27. Desprat, N., A. Richert, …, A. Asnacios. 2005. Creep function of a single living cell. *Biophys. J.* 88:2224–2233.

28. Alcaraz, J., L. Buscemi, …, D. Navajas. 2003. Microrheology of human lung epithelial cells measured by atomic force microscopy. *Biophys. J.* 84:2071–2079.

29. Lau, A. W. C., B. D. Hoffman, …, T. C. Lubensky. 2003. Microrheology, stress fluctuations, and active behavior of living cells. *Phys. Rev. Lett.* 91:198101.

30. Nekrasova, O. E., M. G. Mendez, …, A. A. Minin. 2011. Vimentin intermediate filaments modulate the motility of mitochondria. *Mol. Biol. Cell.* 22:2282–2289.

31. Chang, L., K. Barlan, …, R. D. Goldman. 2009. The dynamic properties of intermediate filaments during organelle transport. *J. Cell Sci.* 122:2914–2923.

32. Gao, Y., and E. Sztul. 2001. A novel interaction of the Golgi complex with the vimentin intermediate filament cytoskeleton. *J. Cell Biol.* 152:877–894.

33. Gao, Y. S., A. Vrielink, …, E. Sztul. 2002. A novel type of regulation of the vimentin intermediate filament cytoskeleton by a Golgi protein. *Eur. J. Cell Biol.* 81:391–401.

34. Styers, M. L., A. P. Kowalczyk, and V. Faundez. 2005. Intermediate filaments and vesicular membrane traffic: the odd couple's first dance? *Traffic.* 6:359–365.

35. Styers, M. L., G. Salazar, …, V. Faundez. 2004. The endo-lysosomal sorting machinery interacts with the intermediate filament cytoskeleton. *Mol. Biol. Cell.* 15:5369–5382.

36. Ehrlicher, A. J., F. Nakamura, …, T. P. Stossel. 2011. Mechanical strain in actin networks regulates FilGAP and integrin binding to filamin A. *Nature.* 478:260–263.

37. Wang, N., J. D. Tytell, and D. E. Ingber. 2009. Mechanotransduction at a distance: mechanically coupling the extracellular matrix with the nucleus. *Nat. Rev. Mol. Cell Biol.* 10:75–82.

38. Fletcher, D. A., and R. D. Mullins. 2010. Cell mechanics and the cytoskeleton. *Nature.* 463:485–492.

39. Ingber, D. E. 2003. Mechanobiology and diseases of mechanotransduction. *Ann. Med.* 35:564–577.

40. Mendez, M. G., S. I. Kojima, and R. D. Goldman. 2010. Vimentin induces changes in cell shape, motility, and adhesion during the epithelial to mesenchymal transition. *FASEB J.* 24:1838–1851.

41. Eckes, B., D. Dogic, …, T. Krieg. 1998. Impaired mechanical stability, migration and contractile capacity in vimentin-deficient fibroblasts. *J. Cell Sci.* 111:1897–1907.

42. Rogel, M. R., P. N. Soni, …, K. M. Ridge. 2011. Vimentin is sufficient and required for wound repair and remodeling in alveolar epithelial cells. *FASEB J.* 25:3873–3883.

43. Koster, S., Y. C. Lin, …, D. A. Weitz. 2010. Nanomechanics of vimentin intermediate filament networks. *Soft Matter.* 6:1910–1914.